



# In Vivo Measurement of Optical Properties of Human Skin for 450–800 nm and 950–1600 nm Wavelengths

Takahiro Kono<sup>1</sup> · Jun Yamada<sup>1</sup>

Received: 1 June 2017 / Accepted: 12 April 2019 / Published online: 26 April 2019  
© The Author(s) 2019

## Abstract

Laser or light-emitting diode therapy has been developed for medical care and skin rejuvenation. Some of these therapies are not only ineffective, but also unsafe. To address these issues, the optical properties of human skin that characterize radiation transfer to the skin have to be clearly understood. In this study, we use in-house instruments to measure the in vivo absorption and scattering coefficients for 198 Japanese participants in visible (450–800 nm) and near-infrared (950–1600 nm) region. The average values and standard deviations of the optical properties are recorded. The effects of age, gender, and body parts on these parameters are analyzed. For the scattering coefficient, the highest value is observed for the inner forearm and the lowest for the region between the thumb and forefinger; females exhibit higher values than males in the visible and some of near-infrared wavelengths; and the value decreases with the age for males in the visible region. In terms of the absorption coefficient, males exhibit higher values than females in the visible region and some of near-infrared wavelength; and the values increase with age in the visible region; the magnitude relations between the body parts differ with the wavelength.

**Keywords** Absorption coefficient · Human skin · Laser therapy · Light therapy · Optical properties · Scattering coefficient

## 1 Introduction

In the medical field, home-use devices [1] that provide laser or light-emitting diodes therapies (laser/light therapies) [2–6] are being studied for use in applications such as subcutaneous tumor ablation and skin rejuvenation. Consequently, there exist many devices that have different specifications in terms of the light wavelength, pulse dura-

---

✉ Takahiro Kono  
na14102@shibaura-it.ac.jp

<sup>1</sup> Department of Mechanical Engineering, Shibaura Institute of Technology, 3-7-5 Toyosu, Koto-ku, Tokyo 135-8548, Japan

tion, and intensity. In order to achieve the desired effect, a proper set of specifications must be selected according to the objective of the therapy. However, this is a complex task as the specifications must be suitable for patients. Misuse or overuse of the home-use devices must not damage the patient's skin. Thus, to ensure safe laser/light therapy, several studies were undertaken to investigate the radiation transferred to the skin [7, 8].

From the optics viewpoint, human skin is an absorption and scattering medium, and the radiation transfer is treated by Eq. 1 [9, 10].

$$\frac{dI(s, \boldsymbol{\Omega})}{ds} = -(\mu_a + \mu_s)I(s, \boldsymbol{\Omega}) + \frac{\mu_s}{4\pi} \int_{4\pi} p(\boldsymbol{\Omega}' \rightarrow \boldsymbol{\Omega})I(s, \boldsymbol{\Omega}')d\boldsymbol{\Omega}', \quad (1)$$

where  $s$  is the coordinate along this direction,  $\boldsymbol{\Omega}$  is a unit vector meaning the propagation direction of radiation, and  $I$  is the intensity of the radiation. There are three optical properties in the radiation transfer equation: the absorption coefficient  $\mu_a$ , scattering coefficient  $\mu_s$ , and scattering phase function  $p$ .

Miller et al. [8] numerically investigated the effect of optical properties reported by Lister et al. [11] on radiation propagation in the skin. They concluded that radiation propagation varied significantly with changes in the optical properties. Therefore, one must consider the differences in optical properties arising from differences in parameters such as skin color, thickness, and patient age to select a proper home-use device for laser/light therapy that ensures that the skin is not damaged and the effect of the laser/light therapy is enhanced. Lister et al. [11] also reiterated the need for further studies involving a large number of racially diverse patients to clarify the definitive optical properties for normal skin.

The final goal of the authors' research program is to understand the laser/light therapy mechanisms and establish safe and sure therapies. As a first step in achieving this goal, in this study, we measure the average values of the optical properties for normal skin and their standard deviation over a wide wavelength. We also clarify the effects of age, gender, and target body parts on the optical properties. Many researchers have measured the optical properties of human skin [11–20]. The methods used the integrating sphere technique [12], diffuse optical spectroscopic imaging (DOSI) [13–16], and the reflection spatial profile measurement (RSPM) [17–20]. Integrating sphere techniques are generally applicable for measuring the optical properties of various absorption and scattering media such as human skin. This method can estimate the optical properties based on the measurement of transmitted radiation using in vitro skin samples, in which the conditions of several properties such as moisture levels and blood differ significantly from those of in vivo skin. The optical properties of such samples might vary from in vivo samples.

Recently, research on noninvasive in vivo measurement methods for the optical properties of human skin are progressing. DOSI and RSPM are the methods for noninvasive in vivo measurement. DOSI is a measurement in the frequency domain utilizing several laser diodes combined with steady-state measurements using a white light. From the measurement results in the frequency domain, the tissue absorption and scattering coefficients at certain diode wavelengths are estimated inversely using a fitting algorithm for diffusion model of radiation transfer. To obtain the scattering

spectrum, a power-law fitting is performed because the particle size distribution of scatters (0.1–10  $\mu\text{m}$ ) in many biological media and phantoms tend to have smooth wavelength dependence, which is well described by a power function, in a wavelength range of 650 nm to 1000 nm. The absorption spectrum is obtained by fitting the measured steady-state broadband reflectance to several absorption coefficients. Cerussi et al. [14] measured the optical properties of normal breast tissue and 58 samples of breast tissue with malignant tumors in near-infrared wavelength ( $\lambda = 650\text{--}1000$  nm) in order to establish an improved basis for optical detection and diagnosis of the malignant tumors. They observed that characteristics of the optical properties differed between the tumorous tissue and healthy tissue. Recently, an adaptation of the DOSI method to measure the continuous spectra of the optical properties of skin in the wavelength range 500–1000 nm was proposed. To demonstrate the new technique, Tseng et al. [15] measured the optical properties of the dorsal forearm and upper inner arm I–VI in the 500–1000 nm wavelength range for six subjects in the Fitzpatrick skin phototypes I–II, III–IV, and V–VI. Hsu et al. [16] measured the optical properties of keloids, normal scars, and uninjured skin in the 500–1000 nm wavelength on 71 subjects to understand the clinical applicability of their measurement system for evaluation of the scar severity and therapeutic response of keloid. They concluded that their method has potential as an object technique for evaluation of keloid scar severity, and it may be a useful tool for tracking the longitudinal response of scars in response to various therapeutic interventions.

RSPM adopts a structured pattern light projected on the skin and measures spatial profile of reflection. The results in the spatial domain, the tissue absorption, and scattering coefficients are estimated inversely using a fitting algorithm for diffusion model of radiation transfer. Saager et al. [18] measured the optical properties of the dorsal forearm and upper inner arm in 450–1000 nm wavelength on 12 subjects ranged in Fitzpatrick skin phototypes I–VI. In their literature, in order to evaluate melanin concentration and distribution thickness *in vivo*, their spatial frequency domain measurements are compared with data obtained from multiphoton microscopy using selective two-photon excited fluorescence of melanin.

The optical properties of normal and diseased skins for diagnosis or treatment of disease in the 450–1000 nm wavelength range are well studied. However, there is no comprehensive study that describes the standard values and standard deviations of the optical properties, which are measured by considering dependent factors such as age, gender, body parts, and individual differences. The analysis of normal skin is important because laser/light therapy is also used in home-use devices for skin rejuvenation. Optical properties must also be analyzed over a wide wavelength range because the devices used in laser/light therapy operate at different wavelengths. Examples of such devices are the 470 nm light-emitting diode [3], 1064 nm Nd:YAG laser [4], and 1550 nm erbium glass lasers [6].

In our previous study, we developed a practical high-performance instrument to measure the optical properties using RSPM [20]. We also developed two instruments for visible ( $\lambda = 450\text{--}800$  nm) and near-infrared ( $\lambda = 950\text{--}1600$  nm) wavelength using the RSPM system. In this study, we measure the optical properties of human skin in 198 Japanese participants to clarify the standard values of absorption and scattering coefficients. We analyze the standard deviation in the individual differences and the

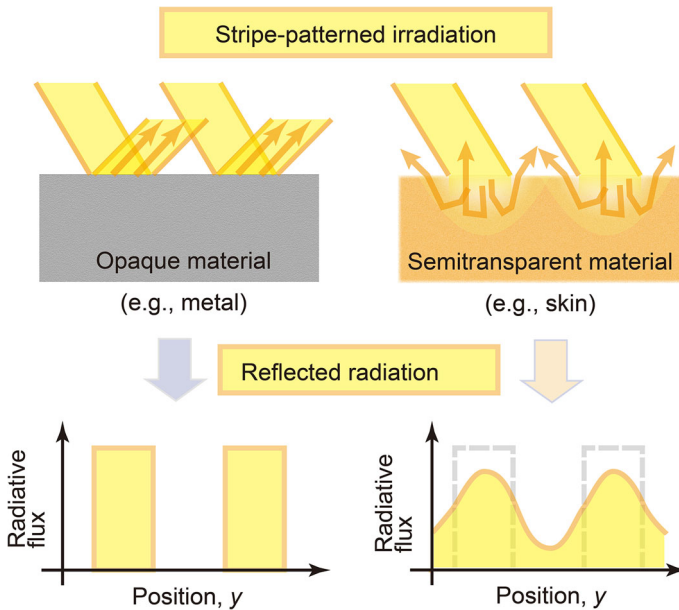


Fig. 1 Reflection by surfaces exposed to stripe-patterned radiation

effect of aging, gender, and body parts on the optical properties in visible and near-infrared wavelength.

## 2 Estimation Method of RSPM

### 2.1 Principle

Figure 1 shows principle of a reflection spatial profile measurement (RSPM). A stripe-patterned radiation irradiated on the skin, in which irradiated portion of uniform radiation and non-irradiated portion are repeated periodically. If the measured material was opaque-like metal, no reflection from the non-irradiated portion would exist because the incident radiation reflected only on the surface of the irradiated portion. On the other hand, since the skin is scattering medium, the incident radiation enters the skin and a part of the radiation propagates in the skin while repeating scattering, so that reflection from the non-irradiated portion exists. The characteristics of the optical properties appear in the spatial profile of the reflected radiation. Therefore, the RSPM can estimate the optical properties using an inverse analysis.

### 2.2 Inverse Analysis Method

The details of this method are provided in Ref. [19]. The skin is regarded as an infinitely wide parallel plane. The optical thickness for the skin tissue is assumed as 20, and the

bottom surface of the skin tissue is assumed as complete absorption because bottom of the skin tissue has no effect on the characteristics of reflection. The top surface is assumed to be smooth, where the reflection on the top surface is calculated by using the Fresnel relations. The refractive index  $n$  of the skin is 1.35–1.55 [21, 22], which varies depending on the moisture content of the skin. Therefore, the refractive index of the skin is assumed as 1.5.

Figure 2 shows the profiles of the reflected radiation intensity by the skin. The vertical axis in Fig. 2 is the relative intensity of the reflected radiation that is the radiation energy flux  $q$  of the irradiation part divided by  $\pi$ . The stripe-patterned irradiation has a 2 mm pitch, in which the width of the irradiated and non-irradiated portions is 1 mm each. The irradiation angle is  $30^\circ$ , and the angle of the measured radiation is normal to the surface. Since the profile of the incident radiation and optical properties of the skin affects the profile of the reflected radiation, the calculated radiation intensity shows a sinusoidal profile. Although the amplitude of the reflected radiation profile is characterized by both the albedo and extinction coefficient, the average intensity of the profile is decided by only the albedo. The behavior of the reflected radiation profile determined the method of inverse analysis for estimating optical properties; the albedo can be estimated firstly using the average of the reflected radiation profile, and then, the extinction coefficient can be estimated using the estimated albedo and the amplitude of the profile, when the model is assumed to be a bulk material ignoring differences in skin layers such as epidermis and dermis. In this study, we analyze the absorption coefficient  $\mu_a$  and scattering coefficient  $\mu_s$ , which are calculated using Eqs. 2 and 3.

$$\beta = \mu_a + \mu_s \quad (2)$$

$$\omega = \frac{\mu_s}{\beta} \quad (3)$$

To estimate the extinction coefficient and albedo using inverse analysis, the scattering phase function must be assigned. The phase function used in this analysis is shown in Fig. 3; this has been taken from a study conducted by one of the authors, Naito et al. [23]. As shown in Fig. 3, there are the measurement data and two Henyey–Greenstein phase functions that approximate the measurement data.

### 2.3 Measurement Setup

Figure 4 shows a schematic diagram for the measurement setup. A halogen lamp is used as the radiation source, and a multi-slit mask is placed next to the lamp to generate the stripe-patterned radiation. The stripe-patterned radiation is projected onto the skin surface through an extended projection lens. The reflected radiation profile perpendicular to the skin is captured by a cooled charge-coupled device (CCD) camera. Since this optical system has a diffraction grating in front of the CCD camera, which means a spectroscopic system, the reflected radiation profile is decomposed into spectral information and recorded using the CCD camera. A sample image taken with this system is also shown in Fig. 4. The vertical profile shows the radiation intensity, while the hori-

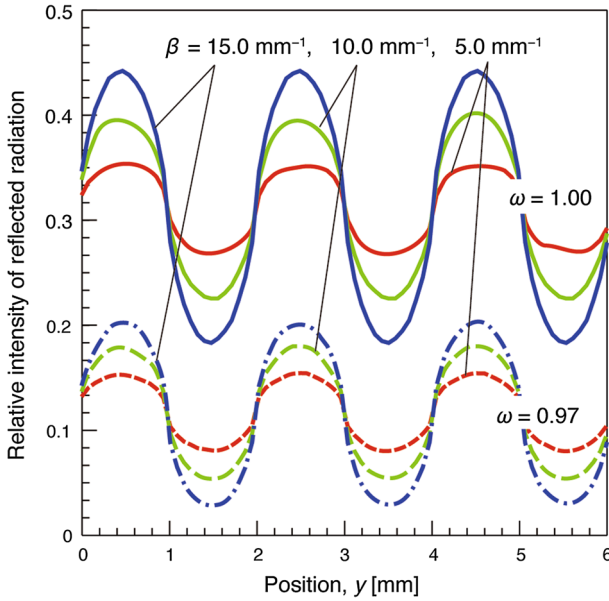


Fig. 2 Calculated intensity profile of reflected radiation

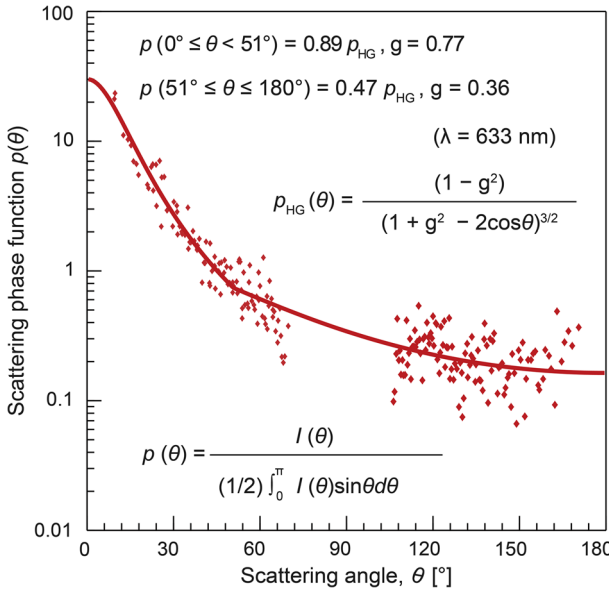
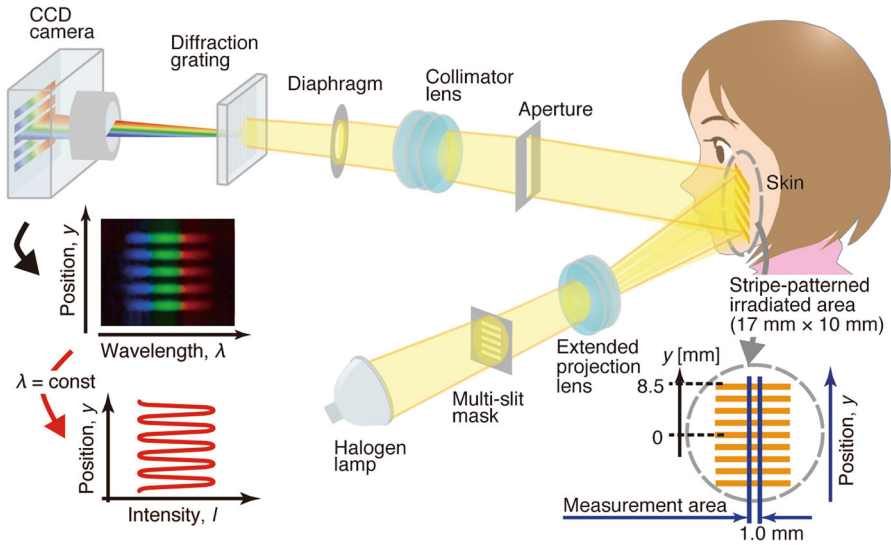


Fig. 3 Scattering phase function of human skin for the inverse method

zontal profile represents the spectral dependence of the reflected intensity. Therefore, only a picture shown in Fig. 4 is used to estimate the spectral optical properties of the human skin. Since this measurement estimates average optical properties within the



**Fig. 4** Schematic of the measurement setup

measurement area (Fig. 4), the skin's local inhomogeneities are smaller than the area averaged.

Two instruments were used to measure the optical properties in addition to the RSPM system. One instrument measured the optical properties in the visible ( $\lambda = 450\text{--}800\text{ nm}$ ) wavelength, while the other operated in the near-infrared ( $\lambda = 950\text{--}1600\text{ nm}$ ) wavelength. The details of the former system are reported in Ref. 20. These instruments differ only in the lens, diffraction grating, and CCD camera, which are adapted to the visible or near-infrared wavelength regions. The optical design was based on our previous study [20].

### 3 Results and Discussions

Measurements were made on the inner forearm, cheek, dorsal surface of the hand, and the region between the thumb and forefinger of the hand for 198 Japanese subjects using the two instruments. The age and gender of the sample population are shown in Table 1. Here,  $N$  refers to the number of subjects.

#### 3.1 Optical Properties of the Skin of the Japanese Participants

Figure 5 shows the average values of the absorption and scattering coefficients for all the subjects and the standard deviation ( $\pm 1\text{ SD}$ ) range for each of them. These data are organized according to the body part, specifically the inner forearm, cheek, dorsal surface of hand, and between thumb and forefinger of the hand. As seen in Fig. 5a, b, for dorsal arm, the range of the absorption coefficients is from  $0.0374\text{ mm}^{-1}$  to

**Table 1** Number of subjects ( $N = 198$ )

Age	Male	Female
20–29	21	23
30–39	13	23
40–49	19	26
50–59	18	18
60–69	14	5
70–79	5	8
80–89	2	3

0.0835  $\text{mm}^{-1}$  for  $\lambda = 650$  nm, and from 0.0376  $\text{mm}^{-1}$  to 0.0705  $\text{mm}^{-1}$  for  $\lambda = 1000$  nm. The range of the scattering coefficients is from 9.68  $\text{mm}^{-1}$  to 11.71  $\text{mm}^{-1}$  for  $\lambda = 650$  nm, and from 6.34  $\text{mm}^{-1}$  to 8.32  $\text{mm}^{-1}$  for  $\lambda = 1000$  nm. In the previous study, the average value of the absorption coefficient of the dorsal arm for skin phototypes III–IV was 0.066  $\text{mm}^{-1}$  for  $\lambda = 650$  nm and 0.0565  $\text{mm}^{-1}$  for  $\lambda = 1000$  nm. The average value of the scattering coefficient was 11.05  $\text{mm}^{-1}$  for  $\lambda = 650$  nm and 6.9  $\text{mm}^{-1}$  for  $\lambda = 1000$  nm [15]. Therefore, our results are in good agreement with the previous study in both the visible and the near-infrared wavelengths.

The standard deviation values take into account the individual differences and provide an idea about the variation of optical properties across normal human skin in Japanese people. This will help other studies to predict the effect of laser/light therapy on the skin with more precision.

### 3.2 Differences in the Optical Properties of Human Skin with Respect to Body Parts

Figure 6 shows the average values of each optical property for all the subjects and body parts. The absorption and scattering coefficient values differ depending on the body part under consideration. In terms of the absorption coefficient (Fig. 6a), the magnitude relationship between the body parts varies with the wavelength. On the other hand, in terms of the scattering coefficient (Fig. 6b), the highest value is observed in the inner forearm, followed by the cheek, dorsal surface of the hand, and the region between the thumb and forefinger of the hand, for all wavelengths.

To determine that there exists a statistically significant difference between them,  $p$  values between the absorption and scattering coefficients of the inner forearm and the region between the thumb and forefinger of the hand were calculated [24] for each wavelength (Fig. 7). The  $p$  value is a probability of the obtained results being extreme or extreme compared to the ones observed, given that the null hypothesis is true. Thus, the smaller the  $p$  value, the more evidence we have for rejecting the null hypothesis. In this study, the  $p$  values are calculated by using a two-tailed Welch's  $t$  test [25, 26] for independent samples. One of the most common tests in statistics is the  $t$  test, used to determine whether the means of two groups are equal to each other. Welch's  $t$  test is an adaptation of Student's  $t$  test, which is more reliable when the two samples have normality, unequal variances and unequal sample sizes. Our measurement results for

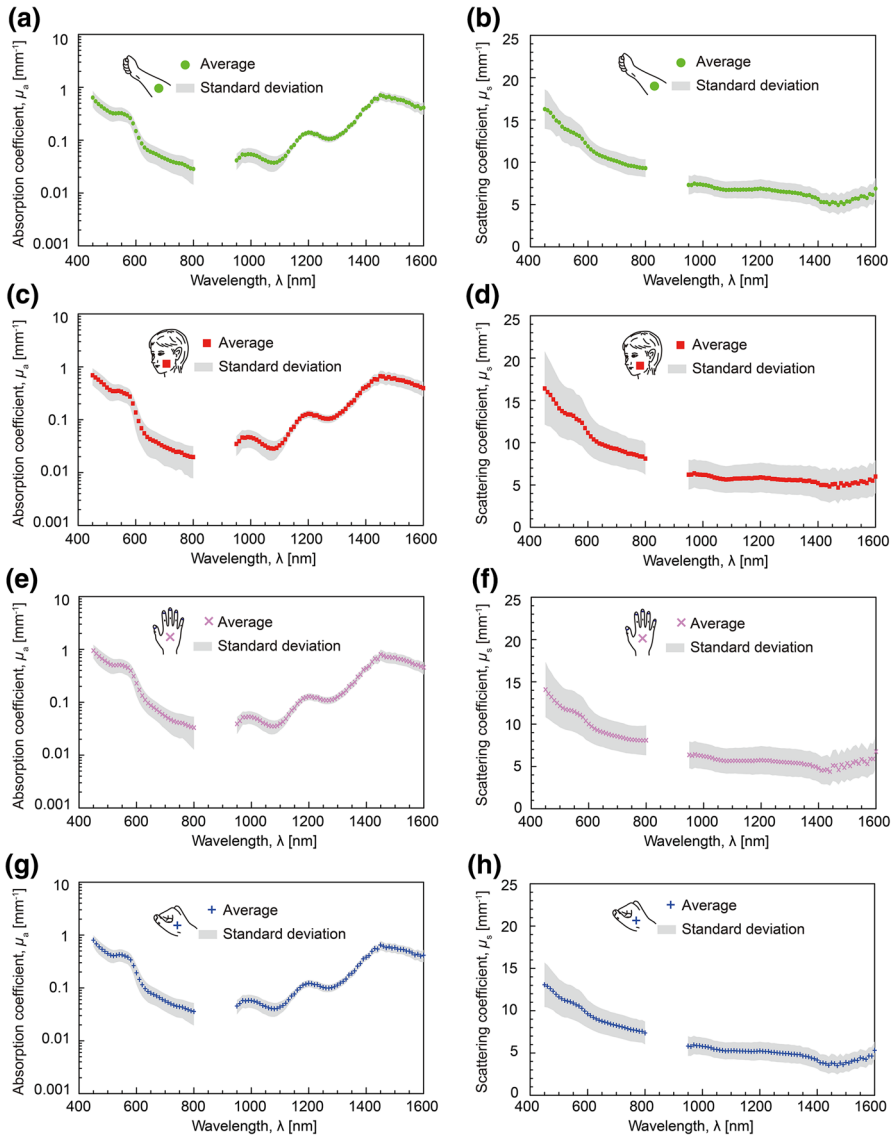


**Fig. 5** Average values and standard deviation range ( $\pm 1$  SD) of the absorption and scattering coefficients for all the subjects, grouped according to the body part—(a, b) inner forearm, (c, d) cheek, (e, f) dorsal surface of the hand, and (g, h) region between the thumb and forefinger of the hand

the body parts had normality, which was confirmed using the Jarque–Bera test [27], and unequal variances, so that we decided to use Welch’s *t* test.

The results show that there is a significant difference in the absorption coefficient for different body parts ( $p < 0.05$ ) in the entire visible wavelength range and almost all the near-infrared wavelengths (Fig. 7a). This is also observed for the scattering coefficient values for all wavelengths (Fig. 7b).

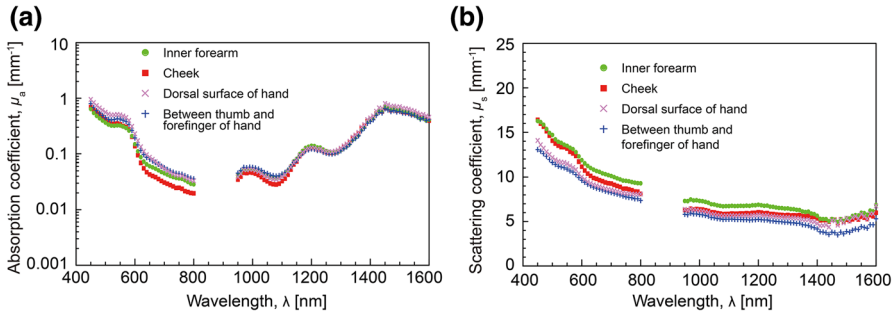


**Fig. 6** Average values of the (a) absorption and (b) scattering coefficients for all the subjects with respect to the body parts

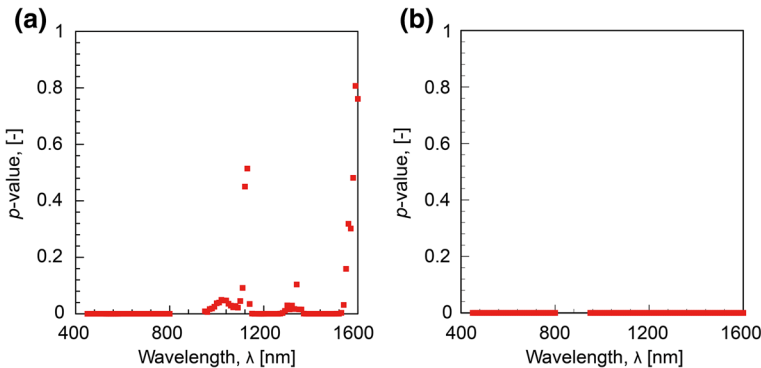


**Fig. 7** Calculated  $p$  values for (a) absorption and (b) scattering coefficient differences between the inner forearm and the region between the thumb and forefinger of the hand at different wavelengths

### 3.3 Differences in the Optical Properties of Human Skin with Respect to Age and Gender

Figure 8 shows the average values of the optical properties of the cheek, categorized on the basis of the age and gender of the participants. Specifically, the groups are males under the age of 40 ( $N = 34$ ), males of age 40 and above ( $N = 58$ ), females under the age of 40 ( $N = 46$ ), and females of age 40 and above ( $N = 60$ ). This categorization ensures that the effect of age is not confused with the effect of gender. Further, in order to obtain only the influence of age, it is necessary to compare in groups of large numbers so that individual differences do not have a significant influence. As seen in Table 1, since the number of people is small and the differences in the number is large when dividing them into every age-group every 10 years, we divided them into two groups, young and elderly, so as not to make much people number difference, and compared them. With respect to the absorption coefficient (Fig. 8a), it is observed that the male groups have higher values than female groups, and older age-groups have higher values than younger groups for the visible wavelength range. On the other hand, in terms of the scattering coefficient (Fig. 8b), the female groups have higher values

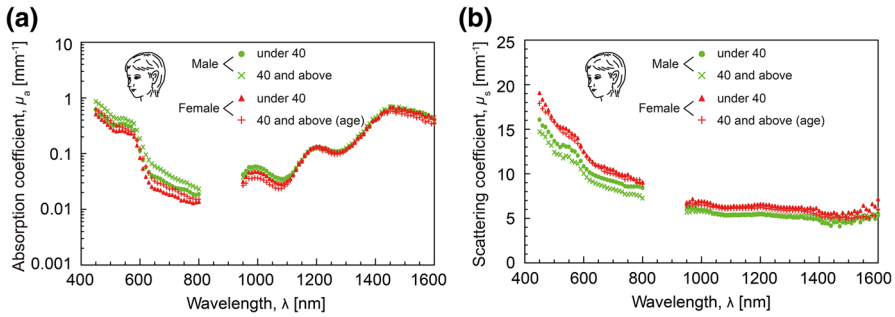


**Fig. 8** Average values of (a) absorption and (b) scattering coefficients for the cheek separated into age and gender groups, males under the age of 40 ( $N = 34$ ), males of age 40 and above ( $N = 58$ ), females under the age of 40 ( $N = 46$ ), and females of age 40 and above ( $N = 60$ )

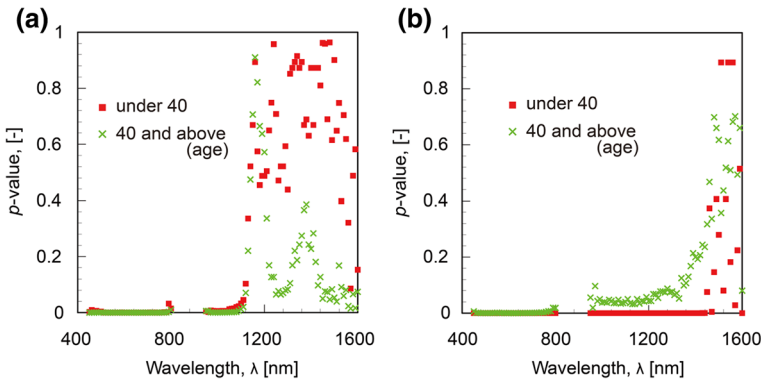


**Fig. 9** Calculated  $p$  values for (a) absorption and (b) scattering coefficient on the basis of gender for each age-group at all wavelengths

than male groups for all wavelengths regardless of their age; the older age-groups have lower values than younger groups for all wavelengths regardless of their gender.

To determine that there exists a statistically significant difference, we calculated the  $p$  values for the male and female groups for each age category using Wilcoxon rank sum test [28] (Fig. 9). Wilcoxon rank sum test is used to investigate the significant difference when the groups to be compared do not have normality. Although majority of the measured data of these four groups had normality, some data sections had no normality, which was confirmed using the Jarque–Bera test. Therefore, the Wilcoxon rank sum test was used for the comparison of these groups. There was a significant difference ( $p < 0.05$ ) in the absorption and scattering coefficients in terms of the gender in the visible wavelength and in some sections of the near-infrared wavelength for both age-groups. We also calculated the  $p$  values for the two age-groups for each gender category. There was a significant difference ( $p < 0.05$ ) in the absorption coefficient with respect to age in the visible wavelength and in some sections of near-infrared wavelength for both gender groups. Moreover, there was a significant difference in the scattering coefficient depending on the age in the visible wavelength for male group.

### 3.4 Factors Affecting Absorption and Scattering Coefficients

The absorption coefficient of the human skin is affected by deoxyhemoglobin, oxy-hemoglobin, melanin, water, and lipid content [11, 29]. Hemoglobin and melanin are dominant on the absorption coefficient in the visible wavelength region, and the water and lipid are dominant in the near-infrared wavelength region. In the visible wavelength region, since the amount of melanin changes due to factors such as sunburn, the absorption coefficient varies depending on age, gender, and body parts. On the other hand, in the near-infrared wavelength region, the content of water does not change greatly depending on age, gender, and body parts. Therefore, it is considered that the measurement results do not change significantly. Their impact on the absorption coefficient could be estimated based on the measurements provided in this study.

On the other hand, the scattering coefficient is affected by the skin structure, collagen fibers, mitochondria, cell walls, nuclei, etc. [11, 30, 31]. The importance of these factors with respect to the scattering coefficient could also be estimated based on the measurements provided in this study. For example, Lee et al. [32] showed that the skin thickness varies between males and females, and between different regions of the body parts. In terms of the thickness of the epidermis, the lowest value was observed in the inner forearm, followed by the cheek and dorsal surface of the hand. Further, females had lower thickness of the epidermis of the cheek than males. When comparing the skin thickness and the measured scattering coefficients, it is revealed that the thinner the skin, the higher the scattering coefficient, both for different body parts and gender. However, in order to elucidate the detailed influence of these factors on the scattering coefficient, we need to consider the structure of the human skin, which has different layers, such as the stratum corneum and stratum spinosum in the epidermis, and the papillary stratum and reticular layer in the dermis, each of which could have different optical properties. We intend to address this issue in our future work and develop a method to measure the optical properties of the layered skin structure.

## 4 Conclusion

In this study, we measured the optical properties of human skin in 198 Japanese people. By analyzing the results, we obtained the standard values and standard deviations of the absorption and scattering coefficients in the visible ( $\lambda = 450\text{--}800$  nm) and near-infrared ( $\lambda = 950\text{--}1600$  nm) wavelengths. We also analyzed the effect of age, gender, and body part on the optical properties. We found statistically significant differences based on these factors in the visible and near-infrared wavelengths. With respect to the absorption coefficient, the magnitude relations between the body parts differ depending on the wavelength; males have higher values than females in the visible region and some sections of the near-infrared wavelength; and the value increases with age in the visible region. With respect to the scattering coefficient, the highest value is observed on the inner forearm and the lowest in the region between the thumb and forefinger of the hand for all wavelengths; females have higher values than males in the visible region and some sections of near-infrared wavelength; and the value decreases with age for males in the visible region.

In summary, although further studies are needed to analyze the variation in layered optical properties, the measurements provided in this study can be used to understand the effect of laser/light therapies and ensure the safety of the customers.

**Funding** This research did not receive any specific grant from funding agencies in the public, commercial, or not-for-profit sectors.

## Compliance with Ethical Standards

**Conflict of interest** The authors declare that they have no conflict of interest.

**Ethical Approval** This article does not contain any studies with humans or animals subjects performed by any of the authors.

**Open Access** This article is distributed under the terms of the Creative Commons Attribution 4.0 International License (<http://creativecommons.org/licenses/by/4.0/>), which permits unrestricted use, distribution, and reproduction in any medium, provided you give appropriate credit to the original author(s) and the source, provide a link to the Creative Commons license, and indicate if changes were made.

## References

1. N.S. Sadick, Y. Harth, J. Cosmet. Laser Ther. **18**, 422–427 (2016). <https://doi.org/10.1080/14764172.2016.1202419>
2. L. Tao, J. Wu, H. Qian, Z. Lu, Y. Li, W. Wang, X. Zhao, P. Tu, R. Yin, L. Xiang, Lasers Med. Sci. **30**, 1977–1983 (2015). <https://doi.org/10.1007/s10103-015-1792-8>
3. M. Figurová, V. Ledecký, M. Karasová, M. Hluchý, A. Trbolová, I. Capík, S. Horňák, P. Reichel, J.M. Bjordal, P. Gál, Photomed. Laser Surg. **34**, 53–55 (2016). <https://doi.org/10.1089/pho.2015.4013>
4. J.H. Shen, C.C. Chang, Y.T. Chen, C.J. Hsieh, H. Huang, B.S. Lin, Ann. Plast. Surg. **77**, S32–S35 (2016). <https://doi.org/10.1097/SAP.0000000000000844>
5. P. Mezzana, V. Maurizio, V. Roberto, J. Cosmet. Laser Ther. **18**, 397–402 (2016). <https://doi.org/10.1080/14764172.2016.1202417>
6. J. Preissig, K. Hamilton, R. Markus, Semin. Plast. Surg. **26**, 109–116 (2012). <https://doi.org/10.1055/s-0032-1329413>
7. J. Wangcun, G. Aguilar, W. Verkruysse, W. Franco, J.S. Nelson, Lasers Surg. Med. **38**, 155–162 (2006). <https://doi.org/10.1002/lsm.20255>
8. S. Miller, K. Mitra, *Proceedings of the SPIE 9706, Optical Interactions with Tissue and Cells XXVII, 97061Q* (2016). <https://doi.org/10.1117/12.2213841>
9. R. Siegel, J.R. Howel, *Thermal Radiation Heat Transfer*, 3rd edn. (Taylor and Francis, New York, 1992), pp. 686–689
10. M.N. Özışık, *Radiative Transfer & Interactions With Conduction & Convection* (Welbel & Peck, New York, 1985), pp. 249–254
11. T. Lister, P.A. Wright, P.H. Chappell, J. Biomed. Opt. **17**, 90901–909011 (2012). <https://doi.org/10.1117/1.JBO.17.9.090901>
12. A.N. Bashkatov, E.A. Genina, V.I. Kochubey, V.V. Tuchin, J. Phys. D Appl. Phys. **38**, 2543 (2005). <https://doi.org/10.1088/0022-3727/38/15/004>
13. F. Bevilacqua, A.J. Berger, A.E. Cerussi, D. Jakubowski, B.J. Tromberg, Appl. Opt. **39**, 6498–6507 (2000). <https://doi.org/10.1364/AO.39.006498>
14. A. Cerussi, N. Shah, D. Hsiang, A. Durkin, J. Butler, B.J. Tromberg, J. Biomed. Opt. **11**, 044005 (2006). <https://doi.org/10.1117/1.2337546>
15. S.H. Tseng, P. Bargo, A. Durkin, N. Kollias, Opt. Express **17**, 14599–14617 (2009). <https://doi.org/10.1364/OE.17.014599>
16. C.K. Hsu, S.Y. Tzeng, C.C. Yang, J.Y. Lee, L.L. Huang, W.R. Chen, M. Hughes, Y.W. Chen, Y.K. Liao, S.H. Tseng, Biomed. Opt. Express **6**, 390–404 (2015). <https://doi.org/10.1364/BOE.6.000390>

17. D.J. Cuccia, F. Bevilacqua, A.J. Durkin, F.R. Ayers, B.J. Tromberg, J. Biomed. Opt. **14**, 024012 (2009). <https://doi.org/10.1117/1.3088140>
18. R.B. Sagger, M. Balu, V. Crosignani, A. Sharif, A.J. Durkin, K.M. Kelly, B.J. Tromberg, J. Biomed. Opt. **20**, 066005 (2015). <https://doi.org/10.1117/1.JBO.20.6.066005>
19. J. Yamada, Y. Arita, A. An, Y. Miura, S. Takata, T. Jpn. Soc. Mech. Eng. Ser. B **74**, 2034–2039 (2008). <https://doi.org/10.1299/kikaib.74.2034>
20. T. Kono, J. Yamada, Jpn. J. Thermophys. Prop. **31**, 72–80 (2017). <https://doi.org/10.2963/jjtp.31.72>
21. M.J.C. Van Gemert, S.L. Jacques, H.J.C.M. Sterenborg, W.M. Star, I.E.E.E. Trans, Biomed. Eng. **36**, 1146–1154 (1989). <https://doi.org/10.1109/10.42108>
22. R.R. Anderson, J.A. Parrish, J. Dermatol. Sci. **77**, 13–19 (1981). <https://doi.org/10.1111/1523-1747.ep12479191>
23. K. Naito, J. Yamada, T. Ogawa, S. Takata, Jpn. J. Thermophys. Prop. **24**, 101–108 (2010). <https://doi.org/10.2963/jjtp.24.101>
24. C. Franco, B.K. Stan, H.H. Heine, O.A. James, P. Martine, *Textbook of Medical Oncology*, 4th edn. (CRC Press, London, 2009), pp. 72–73
25. A.C. Elliott, W.A. Woodward, *Statistical Analysis Quick Reference Guidebook: With SPSS Examples*, 1st edn. (SAGE Publications, Thousand Oaks, 2006), pp. 49–73
26. K.K. Yuen, *Biometrika* **61**, 165–170 (1974). <https://doi.org/10.2307/2334299>
27. C.M. Jarque, A.K. Bera, *Econ. Lett.* **6**, 255–259 (1980). [https://doi.org/10.1016/0165-1765\(80\)90024-5](https://doi.org/10.1016/0165-1765(80)90024-5)
28. J.D. Gibbons, S. Chakraborti, *Nonparametric Statistical Inference*, 4th edn. (Marcel Dekker Inc, New York, 2011), pp. 296–306
29. C.L. Tsai, J.C. Chen, W.J. Wang, J. Med. Biol. Eng. **21**, 7–14 (2001)
30. T. Igarashi, K. Nishino, S.K. Nayar, *Found. Trends@ Comput. Graph. Vis.* **3**, 1–95 (2007). <https://doi.org/10.1561/06000000013>
31. M. Bohnert, R. Walther, T. Roths, J. Honerkamp, *Int. J. Leg. Med.* **119**, 355–362 (2005). <https://doi.org/10.1007/s00414-005-0541-0>
32. Y. Lee, K. Hwang, *Found. Surg. Radiol. Anat.* **24**, 183–189 (2002). <https://doi.org/10.1007/s00276-002-0034-5>

**Publisher's Note** Springer Nature remains neutral with regard to jurisdictional claims in published maps and institutional affiliations.